Hormone Activity of Hydroxylated Polybrominated Diphenyl Ethers on Human Thyroid Receptor-β: *In Vitro* and *In Silico* Investigations

Fei Li,[1] Qing Xie,[1] Xuehua Li,[1] Na Li,[2] Ping Chi,[1] Jingwen Chen,[1] Zijian Wang,[2]* and Ce Hao[3]*

[1]Key Laboratory of Industrial Ecology and Environmental Engineering, School of Environmental Science and Technology, Dalian University of Technology, Dalian, China; [2]State Key Laboratory of Environmental Aquatic Chemistry, Research Center for Eco-environmental Sciences, Chinese Academy of Sciences, Beijing, China; [3]Carbon Research Laboratory, Center for Nano Materials and Science, School of Chemical Engineering, State Key Laboratory of Fine Chemicals, Dalian University of Technology, Dalian, China

Background: Hydroxylated polybrominated diphenyl ethers (HO-PBDEs) may disrupt thyroid hormone status because of their structural similarity to thyroid hormone. However, the molecular mechanisms of interactions with thyroid hormone receptors (TRs) are not fully understood.

Objectives: We investigated the interactions between HO-PBDEs and TRβ to identify critical structural features and physicochemical properties of HO-PBDEs related to their hormone activity, and to develop quantitative structure–activity relationship (QSAR) models for the thyroid hormone activity of HO-PBDEs.

Methods: We used the recombinant two-hybrid yeast assay to determine the hormone activities to TRβ and molecular docking to model the ligand–receptor interaction in the binding site. Based on the mechanism of action, molecular structural descriptors were computed, selected, and employed to characterize the interactions, and finally a QSAR model was constructed. The applicability domain (AD) of the model was assessed by Williams plot.

Results: The 18 HO-PBDEs tested exhibited significantly higher thyroid hormone activities than did PBDEs ($p < 0.05$). Hydrogen bonding was the characteristic interaction between HO-PBDE molecules and TRβ, and aromaticity had a negative effect on the thyroid hormone activity of HO-PBDEs. The developed QSAR model had good robustness, predictive ability, and mechanism interpretability.

Conclusions: Hydrogen bonding and electrostatic interactions between HO-PBDEs and TRβ are important factors governing thyroid hormone activities. The HO-PBDEs with higher ability to accept electrons tend to have weak hydrogen bonding with TRβ and lower thyroid hormone activities.

Key words: application domain, density functional theory, docking, HO-PBDEs, hydroxylated polybrominated diphenyl ethers, PBDEs, quantitative structure–activity relationship, thyroid hormone receptor. *Environ Health Perspect* 118:602–606 (2010). doi:10.1289/ehp.0901457 [Online 17 December 2009]

Polybrominated diphenyl ethers (PBDEs) have become ubiquitous environmental pollutants because of their historical and widespread use as flame retardants, and they have received great attention from ecological health and environmental perspectives (Athanasiadou et al. 2008; He et al. 2008; Lagalante et al. 2009). Most recently, hydroxylated PBDEs (HO-PBDEs) have caused increasing concern because of reports of their natural production and metabolism (Hakk and Letcher 2003; Malmberg et al. 2005; Malmvarn et al. 2005; Mercado-Feliciano and Bigsby 2008; Wan et al. 2009). HO-PBDEs have been detected in the blood of fish, birds, and mammalian species and even in the abiotic environment (Athanasiadou et al. 2008; Cantón et al. 2008; Lacorte and Ikonomou 2009). Recent studies (Dingemans et al. 2008; Qiu et al. 2009) suggest that some of the toxic effects of PBDEs might be due to their HO metabolites.

In vitro tests have shown that certain PBDEs can affect thyroid hormone homeostasis by acting as potent competitors of thyroid hormones for binding to human transthyretin (TTR) and thyroid hormone receptors (TRs) (Cantón et al. 2006; Darnerud et al. 2007; Zhou et al. 2002). For instance, levels of serum thyroxine (T_4) were significantly decreased when rats were exposed to PBDEs (Zhou et al. 2002). The effects of PBDEs on T_4 levels may require metabolic activation because HO-PBDEs, but not the PBDE congeners themselves, behave as ligands for human TTR *in vitro* (Meerts et al. 2000; Qiu et al. 2007). Kitamura et al. (2008) also reported that 4-OH-BDE-90 and 3-OH-BDE-47 markedly inhibited the binding of triiodothyronine (T_3) to TRα and acted as thyroid hormone-like agents. Recently, Kojima et al. (2009) reported that 4-HO-BDE-90 significantly inhibited TRα- and TRβ-mediated transcriptional activity induced by T_3. Consequently, HO-PBDEs have attracted great attention (Routti et al. 2009). However, there is lack of systematic investigation into the mechanisms by which HO-PBDEs interfere with hormonal actions (Zhao et al. 2008).

There are mainly two subtypes of TRs, TRα and TRβ, expressed from two different genes. TRα mediates the effects of thyroid hormones on the heart, in particular on heart rate and rhythm, whereas most actions of the hormones on the liver and other tissues are mediated more through TRβ (Forrest and Vennstrom 2000). The initial step for chemical mode of action is binding to an intracellular receptor (Kavlock et al. 1996). Given the large number of compounds that may bind to the receptors, there is increasing interest in developing computational methods (*in silico*) to predict affinity of compounds with the receptors, including quantitative structure–activity relationships (QSARs) (Du et al. 2008; Valadares et al. 2007). Furthermore, molecular docking and virtual screening have become an integral part of many modern structure-based computational simulations of chemicals (Martinez et al. 2008). Docking methodologies use the knowledge of three-dimensional structure of a receptor in an attempt to optimize the bound ligand or a series of molecules into the active site. Combinational use of docking with QSAR can provide more information on the interaction between the ligand and the receptor (Sippl 2002; Soderholm et al. 2005).

In this study, we applied an integrated *in vitro* and *in silico* approach to evaluate the thyroid hormone–disrupting potency of HO-PBDEs and to identify critical structural elements and physicochemical properties of HO-PBDEs related to their hormone activity. The hormone activities of 18 HO-PBDEs to human TRβ were determined using the recombinant two-hybrid yeast assay. Molecular docking was performed to find the significant ligand–receptor interactions in the binding site of TRβ, which provided a better understanding of interactions between the HO-PBDEs and TRβ. Molecular structural descriptors were computed, selected, and

Address correspondence to J. Chen, School of Environmental Science and Technology, Dalian University of Technology, Linggong Rd. 2, Dalian 116024, P.R. China. Telephone/Fax: 86-411-8470-6269. E-mail: jwchen@dlut.edu.cn

*These authors contributed equally to this work.

Supplemental Material is available online (doi:10.1289/ehp.0901457 via http://dx.doi.org/).

We thank R. Todeschini, B. Herradon, J.M. Navas, and anonymous reviewers for their valuable help.

The study was supported by the National Basic Research Program (2006CB403302), the National Natural Science Foundation of China (20890113), the High Technology Research and Development Program of China (2007AA06Z415), and the Program for Changjiang Scholars and Innovative Research Team in Universities (IRT0813).

The authors declare they have no actual or potential competing financial interests.

Received 13 September 2009; accepted 17 December 2009.

employed to characterize the interactions, and finally we constructed QSAR models. We also assessed the applicability domain (AD) of the QSAR model.

Materials and Methods

Chemicals. We selected 18 HO-PBDEs for the present study [see Supplemental Material, Figure S1 (doi:10.1289/ehp.0901457)]; most have been detected in environmental/biological samples (Malmberg et al. 2005; Qiu et al. 2007). The HO-PBDEs congeners (> 97% purity) were purchased from AccuStandard (New Haven, CT, USA). 3,3′,5-Triiodothyronine (T_3; 95% purity), dimethyl sulfoxide (DMSO; GC, 99.5% purity), *o*-nitrophenyl β-D-galactopyranoside (*o*-NPG; ≥ 98% purity), sodium dodecyl sulfate (99% purity), leucine (99% purity), tryptophan (99% purity), yeast-based nitrogen (99% purity), and β-mercaptoethanol (99% purity) were purchased from Sigma Chemical Company (St. Louis, MO, USA). Stock solutions of HO-PBDEs were prepared in DMSO.

Recombinant two-hybrid yeast assay and statistical analysis. The recombinant two-hybrid yeast system employed a yeast cell transformed with the human TRβ plasmid, coactive plasmid, and the reporter gene expressing β-galactosidase (Li et al. 2008). We examined the specificity of the yeast two-hybrid assay for TRβ ligand using DMSO (control), T_3, and other steroid hormones. T_3 induced β-galactosidase activity, whereas 17β-estradiol, dihydrotestosterone, and progesterone did not. Thus, the recombinant two-hybrid yeast assay was highly specific for TRβ ligand without cross-talk to other receptor agonists.

We performed the recombinant two-hybrid yeast assay as described previously by Li et al. (2008). Briefly, yeast transformants were grown overnight at 30°C, with vigorous orbital shaking (130 rpm). For the assay, exponentially growing overnight cultures were diluted with synthetic dextrose/leucine/tryptamine medium to an optical density at 600 nm (OD_{600}) of 0.75. All the samples were determined at least in triplicate. Each triplicate included a positive control (T_3) and a negative control (DMSO). Each tested chemical was serially diluted in DMSO for a total of 7–11 concentrations. Serial dilutions (5-μL steps) were combined with 995 μL medium containing 5×10^3 yeast cells/mL, resulting in a test culture in which the volume of DMSO did not exceed 0.5% of the total volume. For each test culture, 200 μL was transferred into a well of the 96-well plate and incubated at 30°C with vigorous orbital shaking (800 rpm) on a titer plate shaker (TITRAMAX 1000; Heidolph Instruments GmbH, Hamburg, Germany) for 2 hr, and the cell density of the culture was measured at OD_{600} (GENios A-5002; Tecan Austria GmbH, Salzburg, Austria). Then, 50 μL test culture was transferred to a new 96-well plate, and after addition of 120 μL Z-buffer (21.51 g/L $Na_2HPO_4 \cdot 12H_2O$; 6.22 g/L $NaH_2PO_4 \cdot 2H_2O$; 0.75 g/L KCl; 0.25 g/L $MgSO_4 \cdot 7H_2O$) and 20 μL chloroform, the cultures were carefully mixed and preincubated for 10 min at 30°C and 13,000 rpm. The enzyme reaction was started by adding 40 μL *o*-NPG (13.3 mM, dissolved in yeast-based buffer). The assay culture was further incubated at 30°C for 1 hr. Finally, the reactions were terminated by the addition of 100 μL sodium carbonate (1 M). The resulting absorption was measured at 420 nm. The β-galactosidase activity (*U*) was calculated according to the following equation:

$$U = \frac{OD_{420} - OD'_{420}}{t \times V \times OD_{600}} \times D, \qquad [1]$$

where *U* is the activity of β-galactosidase, *t* is the incubation duration of the enzyme reaction, *V* is the volume of the test culture, *D* is the diluting factor (6.6), OD_{600} is the cell density measured at 600 nm, and OD_{420} and OD'_{420} are the cell density of the enzymic reaction supernatant and the blank, respectively, measured at 420 nm.

The dose–response curves for *U* of the tested compounds were fitted by iterative four-parameter curve fit method using SigmaPlot, version 10.0 (Systat Software Inc., Chicago, IL, USA). The concentration inducing 20% of the maximum effect (REC_{20}) value was calculated from the fitted dose–response curves. We evaluated the statistical significance of differences by analysis of variance (we considered $p < 0.05$ significant).

Molecular docking. We adapted the CDOCKER algorithm to find the binding mode for HO-PBDEs to TRβ. CDOCKER is an implementation of a CHARMM (Chemistry at HARvard Macromolecular Mechanics)-based docking tool that has been shown to be viable (Wu et al. 2003). It has been incorporated into Discovery Studio 2.1 (Accelrys Software Inc., San Diego, CA) through the Dock Ligands (CDOCKER) protocol. We extracted the crystal structure of TRβ (Thyroid receptor beta1 in complex with a beta-selective ligand; PDB ID 1NAX) from the RCSB Protein Data Bank [RCSB (Research Collaboratory for Structural Bioinformatics) PDB; http://www.rcsb.org/pdb]. In CDOCKER, random ligand conformations were generated from the initial ligand structure through high-temperature molecular dynamics followed by random rotations. Then, the random conformations were refined by grid-based simulated annealing, which makes the results more accurate. The CDOCKER interaction energy between the ligand and TRβ ($E_{binding}$) was then computed. The docking analysis provided insights into the interactions between the ligands and the receptor, which facilitated the selection of appropriate molecular parameters to characterize the interactions in the QSAR studies.

Molecular structural descriptor generation and QSAR development. We hypothesized that the thyroid hormone activities of HO-PBDEs were dependent on *a*) the partition of the compounds between water and the biophase, and *b*) the interaction between the ligands and the receptor TRβ. Thus, 12 theoretical parameters were computed and selected to characterize the processes: the logarithm of octanol/water partition coefficient ($\log K_{ow}$), average molecular polarizability (α), molecular volume (*V*), dipole moment (μ), energy of the highest occupied molecular orbital (E_{HOMO}), energy of the lowest unoccupied molecular orbital (E_{LUMO}), formal charge on hydroxyl hydrogen atoms (q_{OH}), formal charge on hydroxyl oxygen atoms ($q_{\underline{O}H}$), formal charge on ether oxygen atoms (q_O), electrophilicity index (ω), harmonic oscillator model of aromaticity index (I_A), and the number of bromine atoms (n_{Br}) [see also Supplemental Material, Table S1 (doi:10.1289/ehp.0901457)]. We purposely selected $\log K_{ow}$ to describe the partition process. The parameters *V*, n_{Br}, α, and μ also partly describe partition because many of these parameters correlate with $\log K_{ow}$ (Nguyen et al. 2005). The parameters E_{HOMO}, E_{LUMO}, q_{OH}, $q_{\underline{O}H}$, q_O, ω, and I_A were purposely selected to describe the intermolecular electrostatic interactions between the ligands and TRβ. The quantum chemical parameters E_{HOMO}, E_{LUMO}, q_{OH}, $q_{\underline{O}H}$, and q_O proved successful in many QSAR studies for characterizing intermolecular electrostatic interactions (Colosi et al. 2006). ω measures the ability of a compound to soak up electrons. The relative binding affinity of some estrogen derivatives correlated strongly with ω (Chattaraj 2006). The aromaticity of compounds (I_A) may influence their noncovalent interactions with the receptor, and I_A has been used to characterize halogenated biphenyls (Alonso et al. 2008).

We computed $\log K_{ow}$ values using the EPI Suite, version 4.0 (U.S. Environmental Protection Agency 2009). *V* (defined as the volume inside a contour of 0.001 electrons/bohr^3 density) and the quantum chemical parameters were computed by the Gaussian 03 programs (Frisch et al. 2004). Initial geometries of HO-PBDEs were preoptimized by semiempirical PM3 Hamiltonian and then optimized by density functional theory at the B3LYP/6-311+G(d,p) level. Frequency analysis was performed on the optimized geometries to ensure the systems had no imaginary vibration frequencies. I_A was calculated by DRAGON software (Todeschini and Consonni 2000).

The 18 HO-PBDEs were randomly divided into a training set (80%) and a validation set (20%), as listed in Table 1. Partial least squares (PLS) regression was performed in

developing the model because PLS can analyze data with strongly collinear, noisy, and numerous predictor variables (Wold et al. 2001). We used Simca-S (version 6.0; Umetri AB, Umea, Sweden) for the PLS analysis. Simca-S uses leave-many-out cross-validation to determine the number of PLS components (A). Cross-validation simulates how well a model predicts new data and gives a statistical fraction of the total variation of the dependent variables that can be predicted by all the extracted components (Q^2_{CUM}) for the final model. The PLS analysis was performed repeatedly to eliminate redundant molecular structural parameters, as done in our previous studies (Chen et al. 2004). Model predictability was evaluated by external validation, which was characterized by the determination coefficient (R^2), root mean square error (RMSE), and external explained variance (Q^2_{EXT}), which are defined as follows (Schüürmann et al. 2008):

$$R^2 = 1 - \frac{\sum_{i=1}^{n} (y_i^{fit} - y_i)^2}{\sum_{i=1}^{n} (y_i - \bar{y})^2}, \quad [2]$$

$$RMSE = \sqrt{\frac{\sum_{i=1}^{n} (y_i - \hat{y}_i)^2}{n}}, \quad [3]$$

$$Q^2_{EXT} = 1 - \frac{\sum_{i=1}^{n_{EXT}} (y_{i-} \hat{y}_i)^2}{\sum_{i=1}^{n_{EXT}} (y_i - \bar{y}_{EXT})^2}, \quad [4]$$

where y_i^{fit} is the fitted –logREC_{20} value of the ith compound; $\bar{y}$ is the average response value in the training set; y_i and $\hat{y}_i$ are the observed and predicted values for the ith compound, respectively; $\bar{y}_{EXT}$ is the average response value of the validation set; n is the number of compounds in the training set; and n_{EXT} is the number of compounds in the validation set.

We assessed the AD of the developed QSAR model using the Williams plot, that is, the plot of standardized residuals (σ) versus leverage (hat diagonal) values (h_i) (Eriksson et al. 2003). We calculated σ as follows:

$$\sigma = \frac{y_i - \hat{y}_i}{\sqrt{\frac{\sum_{i=1}^{n} (y_i - \hat{y}_i)^2}{(n-1)}}}, \quad [5]$$

where y_i and $\hat{y}_i$ are the observed and predicted values for the ith compound, respectively, and n is the number of compounds in the training set.

The h_i value of a chemical in the original variable space and the warning leverage value (h^*) are defined as follows:

$$h_i = x_i^T (X^T X)^{-1} x_i \; (i = 1, \ldots, n), \quad [6]$$

$$h^* = 3(p + 1)/n, \quad [7]$$

where x_i is the descriptor vector of the considered compound, X is the model matrix derived from the training set descriptor values, and p is the number of predictor variables.

Results and Discussion

Thyroid hormone activity determined by recombined yeast. Based on a plot of U versus log T_3 concentrations, the maximal induction of T_3 was achieved at 1.0×10^{-6} M [see Supplemental Material, Figure S2 (doi:10.1289/ehp.0901457)]. From the dose–response curve, the median effective concentration value of T_3 was 1.4×10^{-7} M, which was similar to that reported by Li et al. (2008). The 18 tested HO-PBDEs induced β-galactosidase activity in a concentration-dependent manner in the concentration range from 10^{-11} to 10^{-6} M (see Supplemental Material, Figure S3). Supplemental Material, Table S2 lists the determined REC_{20} values for the 18 HO-PBDEs.

With 2×10^{-7} M of the tested compounds, the PBDEs showed no significant β-galactosidase activity compared with DMSO, and HO-PBDEs exhibited significant activity [$p < 0.05$; see Supplemental Material, Figure S4 (doi:10.1289/ehp.0901457)]. Previous studies (Hamers et al. 2008; Meerts et al. 2000) indicated that HO metabolites of PBDEs could compete with T_4 for binding to TTR and exert thyroid hormone activity. Kitamura et al. (2008) reported that 4-OH-BDE-90 and 3-OH-BDE-47 markedly inhibited the binding of T_3 to TRα and acted as thyroid hormone-like agents. Kojima et al. (2009) reported that 4-HO-BDE-90 significantly inhibited TRα- and TRβ-mediated transcriptional activity induced by T_3. Thus, with respect to the observed thyroid hormone activity of HO-PBDEs, our results are consistent with previous findings.

Docking analysis. Figure 1 shows the docking view of T_3 and representative HO-PBDEs and PBDEs (4-OH-BDE-42, 4′-OH-BDE-17, and BDE-116) in the binding site of TRβ. At the deep end of the pocket, Arg282 and Ile275 serve as anchoring points for the ligands. The ligands also interact with the second polar region within the binding pocket, Leu341. We observed hydrogen bonding to be a characteristic interaction. As shown in Figure 1B and C, there are mainly two types of hydrogen bonds: those formed between the hydroxyl oxygen of HO-PBDEs and the hydrogen of Arg282 and Ile276, and those between the hydroxyl hydrogen of HO-PBDEs and the carbonyl oxygen of Leu341. However, for BDE-116, we could find no hydrogen bonds with the amino acid residues in TRβ. We also observed π–π interactions between the phenyl of HO-PBDEs and Phe272, Phe442, and Phe455.

The ligand–receptor binding energy ($E_{binding}$) of the 18 HO-PBDEs is listed in Table 1. As shown in Figure 2, we obtained a simple linear free energy relationship between –logREC_{20} and $E_{binding}$, further proving that binding to TRβ is the key step for the HO-PBDEs to exert their thyroid hormone activity. However $E_{binding}$ itself was not a good predictor for –logREC_{20}, as indicated by the big prediction residuals for some HO-PBDEs (Figure 2). This was expected because $E_{binding}$ values calculated by CDOCKER differed from the real binding energy because the environmental factors (e.g., solvents, pH, and ions) were not considered in the modeling, and the ability of β-galactosidase expression for different HO-PBDEs may differ.

Table 1. –logREC_{20} and $E_{binding}$ values for selected compounds.

Compound	–logREC_{20} Observed	–logREC_{20} Predicted	–logREC_{20} Residual	$E_{binding}$ (kJ/mol)
3′-OH-BDE-7[a]	7.64	7.03	0.61	–35.3
4′-OH-BDE-17	8.66	9.05	–0.39	–39.8
3′-OH-BDE-28	7.28	7.75	–0.47	–38.9
2′-OH-BDE-28	8.07	7.95	0.12	–35.8
4-OH-BDE-42	9.72	8.90	0.82	–43.7
4′-OH-BDE-49	7.87	8.31	–0.44	–43.6
3-OH-BDE-47	8.77	8.91	–0.14	–40.0
5-OH-BDE-47[a]	8.44	9.18	–0.74	–40.2
6-OH-BDE-47[a]	10.43	9.85	0.58	–38.8
4-OH-BDE-90	7.63	7.96	–0.33	–41.3
6-OH-BDE-85	9.77	9.79	–0.02	–44.3
6-OH-BDE-87[a]	9.29	9.65	–0.36	–42.0
6-OH-BDE-82	10.44	10.55	–0.11	–44.2
6′-OH-BDE-99	9.62	9.93	–0.31	–39.6
5′-OH-BDE-99	10.34	9.73	0.61	–44.4
6-OH-BDE-157	12.20	11.97	0.23	–46.3
6-OH-BDE-140	11.31	11.80	–0.49	–47.8
3′-OH-BDE-154	10.76	9.91	0.85	–42.0
BDE-30	< 6.70			–37.0
BDE-116	< 6.70			–34.4

[a]Compound selected to form the external validation set.

Thus, it is necessary to develop multiparameter QSAR models for –logREC_{20} prediction.

Development, validation, and AD of the QSAR. PLS analysis with –logREC_{20} as the dependent variable and the molecular structural parameters as predictor variables resulted in the following optimal QSAR model:

$$-\log REC_{20} = 5.73 \times 10 + 8.01 \times 10^{-1}\, n_{Br} + 9.62 \times 10^{-1} \log K_{ow} - 4.95 \times 10\, I_A + 2.84\, E_{LUMO} - 1.66\, \omega + 3.26 \times 10^{-2}\, \mu^2,$$

where $n = 14$, $A = 3$, $R^2 = 0.913$, $Q^2_{CUM} = 0.873$, RMSE (training set) = 0.418, $n_{EXT} = 4$, $Q^2_{EXT} = 0.500$, and RMSE (validation set) = 0.731 ($p < 0.0001$).

Q^2_{CUM} of the QSAR was as high as 0.873, implying good robustness of the model. The differences between R^2 and Q^2_{CUM} did not exceed 0.3, indicating no overfitting in the model (Golbraikh and Tropsha 2002). Figure 3 shows that the predicted –logREC_{20} values are consistent with the observed values for both the validation and training sets. The model has good predictive abilities, as indicated by Q^2_{EXT} = 0.500 and RMSE = 0.731.

The AD is shown by the Williams plot (Figure 4); h_i values of all the compounds in the training and validation sets were lower than the warning value (h^* = 1.500). Thus, none of the compounds are particularly influential in the model space, and the training set has great representativeness. The standardized residuals of all the compounds in the training and validation sets are < 3, so there are no outliers in the developed QSAR model. Considering the mechanism of action, we can infer that the developed QSAR model can be used to predict thyroid hormone activity on TRβ of other HO-PBDEs similar to those used in the present study. To discriminate between active and inactive compounds (e.g., PBDEs and HO-PBDEs), discriminant models should be developed in further studies.

Mechanistic implication of the developed model. The developed PLS model extracted on three PLS components loaded primarily on six predictor variables. Values of the variable importance in the projection (VIP) and PLS weights (W^*) are listed in Table 2. From the W^* values, one can see how the predictor variables and the response variable combine in the projections (PLS components) and how they relate to each other.

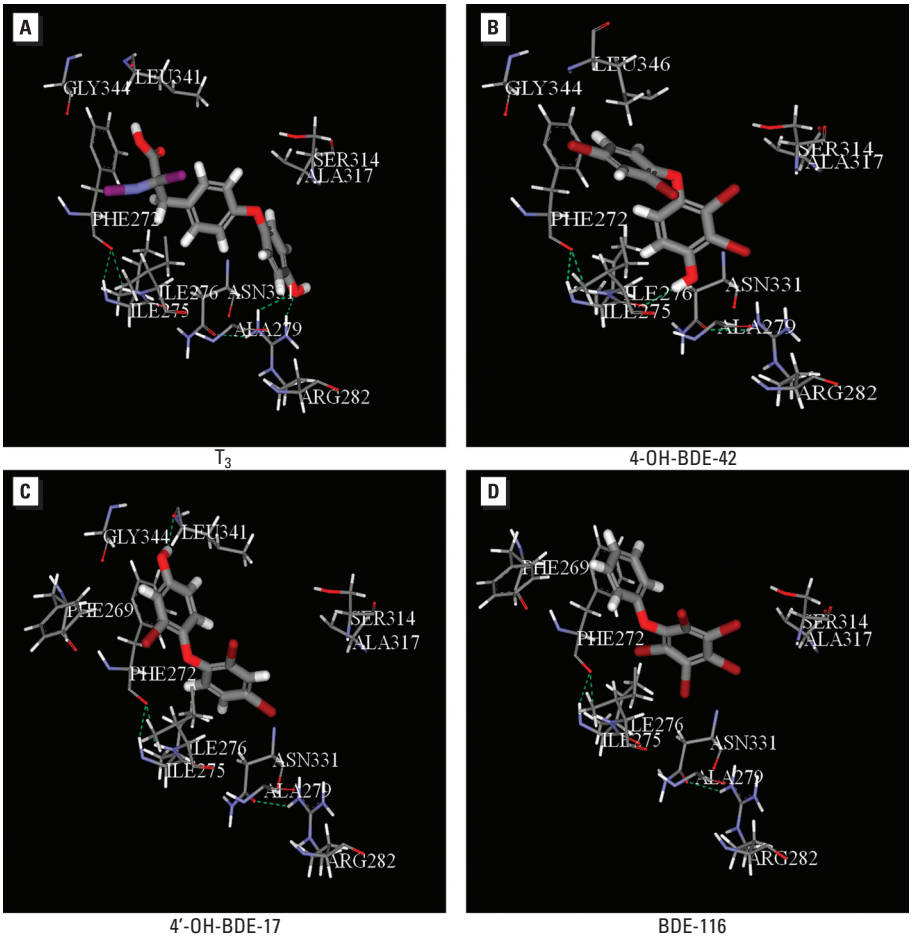

Figure 1. Docking views of T_3 (*A*), 4-OH-BDE-42 (*B*), 4′-OH-BDE-17 (*C*), and BDE-116 (*D*) at the TRβ binding site. Green dashed lines indicate hydrogen bonds between HO-PBDEs and amino acid residues, gray is carbon, red is oxygen, blue is nitrogen, purple is iodine, and white is hydrogen.

The first PLS component (W^*c[1]) is loaded primarily on three descriptors, n_{Br}, logK_{ow}, and I_A (Table 2). These three descriptors remarkably govern –logREC_{20} values, as indicated by their large VIP values among the predictor variables. The coefficients in the QSAR model indicate that –logREC_{20} values of HO-PBDEs increase with n_{Br} and logK_{ow} values but decrease with increasing I_A values. The observation is reasonable because logK_{ow} correlates with n_{Br} positively (r = 0.999,

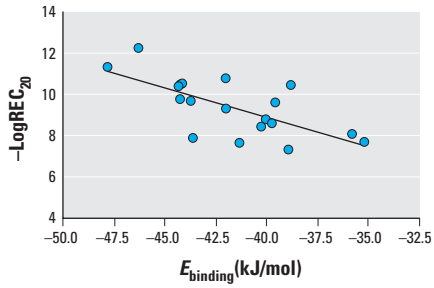

Figure 2. Plot of observed –logREC_{20} versus the $E_{binding}$. R = 0.685; $p < 0.02$.

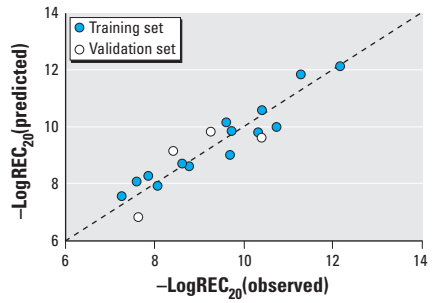

Figure 3. Plot of predicted versus observed –logREC_{20} values for both the training set (R^2_Y = 0.913; RMSE = 0.418) and the validation set (Q^2_{EXT} = 0.500; RMSE = 0.731).

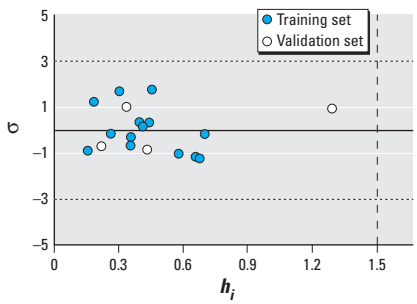

Figure 4. Williams plot showing AD of the developed QSAR model (see also Equations 5 and 6). The vertical dashed line indicates that $h_i = h^*$ = 1.500.

Table 2. VIP values and PLS weights for the optimal PLS model.

Variable	VIP	W^*c[1]	W^*c[2]	W^*c[3]
n_{Br}	1.093	0.487	0.194	0.585
LogK_{ow}	1.091	0.487	0.191	0.581
I_A	1.022	–0.420	–0.589	–0.246
E_{LUMO}	0.980	–0.387	0.469	0.615
ω	0.979	0.392	–0.451	–0.592
μ^2	0.806	0.215	0.428	–0.345

$p < 0.001$) and because HO-PBDEs with large logK_{ow} and n_{Br} values tend to partition into the biophase (yeast cells). The harmonic oscillator model of aromaticity index (I_A) may characterize the noncovalent interactions with TRβ. The deviation from planarity of an aromatic ring is a structural measurement of aromaticity: The higher the planarity, the higher the π electron delocalization and the higher the aromaticity (Alonso et al. 2008). Even for a single ring of polychlorinated biphenyl, aromaticity varied with the number of chlorine atoms (Alonso et al. 2008). Thus, the involvement of I_A in the QSAR model may imply the effects of planarity (or nonplanarity) of HO-PBDE molecules on thyroid hormone activity. According to the QSAR model, I_A plays a negative effect on thyroid hormone activity ($n = 18$; $r = 0.66$; $p < 0.005$). $E_{binding}$ also correlates positively with I_A values ($n = 18$; $r = 0.54$; $p < 0.05$).

The second PLS component (W^*c[2]) is loaded primarily on I_A, E_{LUMO}, ω, and μ^2, and the third PLS component (W^*c[3]) is loaded primarily on n_{Br}, logK_{ow}, E_{LUMO}, and ω. E_{LUMO} itself has a negative value and measures the ability of a molecule to accept electrons. The docking analysis showed that hydrogen bonds were the characteristic interactions between the hydroxyl oxygen of HO-PBDEs and the hydrogen of Arg282 and Ile276. Because HO-PBDE molecules with lower E_{LUMO} values tend to accept electrons easily, accept protons with difficulty, and accordingly form the hydrogen bonds with difficulty, the developed PLS model shows that –logREC_{20} increases with E_{LUMO} values. Likewise, because ω measures the ability of a molecule to soak up electrons (Chattaraj 2006), in the developed PLS model –logREC_{20} increases with decreasing ω values. Finally, μ measures the dipole–dipole and dipole-induced interactions between interacting molecules (Hurth et al. 2004), so HO-PBDEs with large μ values may exhibit strong dipole–dipole interactions with the receptor (TRβ), leading to large –logREC_{20} values.

Conclusion

We determined thyroid hormone activities of selected HO-PBDEs by the recombinant two-hybrid yeast assay. Docking analysis indicated that hydrogen bonding and electrostatic interactions are the key steps for HO-PBDEs to exert thyroid hormone activities. We developed a QSAR to characterize the interactions and model the thyroid hormone activities. The HO-PBDEs with higher ability to accept electrons (as indicated by E_{LUMO} and ω) tend to have weak hydrogen bonding with the receptor and lower thyroid hormone activities. The developed QSAR model has good robustness, predictive ability, and mechanism interpretability.

References

Alonso M, Casado S, Miranda C, Tarazona JV, Navas JM, Herradon B. 2008. Decabromobiphenyl (PBB-209) activates the aryl hydrocarbon receptor while decachlorobiphenyl (PCB-209) is inactive: experimental evidence and computational rationalization of the different behavior of some halogenated biphenyls. Chem Res Toxicol 21:643–658.

Athanasiadou M, Cuadra SN, Marsh G, Bergman A, Jakobsson K. 2008. Polybrominated diphenyl ethers (PBDEs) and bioaccumulative hydroxylated PBDE metabolites in young humans from Managua, Nicaragua. Environ Health Perspect 116:400–408.

Cantón RF, Sanderson JT, Nijmeijer S, Bergman A, Letcher RJ, van den Berg M. 2006. In vitro effects of brominated flame retardants and metabolites on CYP17 catalytic activity: a novel mechanism of action? Toxicol Appl Pharmacol 216:274–281.

Cantón RF, Scholten DEA, Marsh G, De Jong PC, van den Berg M. 2008. Inhibition of human placental aromatase activity by hydroxylated polybrominated diphenyl ethers (OH-PBDEs). Toxicol Appl Pharmacol 227:68–75.

Chattaraj PK, Sarkar U, Roy DR. 2006. Electrophilicity index. Chem Rev 106:2065–2091.

Chen JW, Harner T, Ding GH, Quan X, Schramm KW, Kettrup A. 2004. Universal predictive models on octanol-air partition coefficients at different temperatures for persistent organic pollutants. Environ Toxicol Chem 23:2309–2317.

Colosi LM, Huang QG, Weber WJ. 2006. Quantitative structure-activity relationship based quantification of the impacts of enzyme-substrate binding on rates of peroxidase-mediated reactions of estrogenic phenolic chemicals. J Am Chem Soc 128:4041–4047.

Darnerud PO, Aune M, Larsson L, Hallgren S. 2007. Plasma PBDE and thyroxine levels in rats exposed to Bromkal or BDE-47. Chemosphere 67:386–392.

Dingemans MML, de Groot A, van Kleef RGDM, Bergman A, van den Berg M, Vijverberg HPM, et al. 2008. Hydroxylation increases the neurotoxic potential of BDE-47 to affect exocytosis and calcium homeostasis in PC12 cells. Environ Health Perspect 116:637–643.

Du J, Qin J, Liu HX, Yao XJ. 2008. 3D-QSAR and molecular docking studies of selective agonists for the thyroid hormone receptor beta. J Mol Graph Model 27:95–104.

Eriksson L, Jaworska J, Worth AP, Cronin MTD, McDowell RM, Gramatica P. 2003. Methods for reliability and uncertainty assessment and for applicability evaluations of classification- and regression-based QSARs. Environ Health Perspect 111:1361–1375.

Forrest D, Vennstrom B. 2000. Functions of thyroid hormone receptors in mice. Thyroid 10:41–52.

Frisch MJ, Trucks GW, Schlegel HB, Scuseria GE, Robb MA, Cheeseman JR, et al. 2004. Gaussian 03, Revision C.02. Wallingford, CT:Gaussian, Inc.

Golbraikh A, Tropsha A. 2002. Beware of q^2! J Mol Graph Model 20:269–276.

Hakk H, Letcher RJ. 2003. Metabolism in the toxicokinetics and fate of brominated flame retardants—a review. Environ Int 29:801–828.

Hamers T, Kamstra JH, Sonneveld E, Murk AJ, Visser TJ, Van Velzen MJM, et al. 2008. Biotransformation of brominated flame retardants into potentially endocrine-disrupting metabolites, with special attention to 2,2′,4,4′-tetrabromodiphenyl ether (BDE-47). Mol Nutr Food Res 52:284–298.

He Y, Murphy MB, Yu RMK, Lam MHW, Hecker M, Giesy JP, et al. 2008. Effects of 20 PBDE metabolites on steroidogenesis in the H295R cell line. Toxicol Lett 176:230–238.

Hurth KM, Nilges MJ, Carlson KE, Tamrazi A, Belford RL, Katzenellenbogen JA. 2004. Ligand-induced changes in estrogen receptor conformation as measured by site-directed spin labeling. Biochemistry 43:1891–1907.

Kavlock RJ, Daston GP, DeRosa C, FennerCrisp P, Gray LE, Kaattari S, et al. 1996. Research needs for the risk assessment of health and environmental effects of endocrine disruptors: a report of the U.S. EPA–sponsored workshop. Environ Health Perspect 104:715–740.

Kitamura S, Shinohara S, Iwase E, Sugihara K, Uramaru N, Shigematsu H, et al. 2008. Affinity for thyroid hormone and estrogen receptors of hydroxylated polybrominated diphenyl ethers. J Health Sci 54:607–614.

Kojima H, Takeuchi S, Uramaru N, Sugihara K, Yoshida T, Kitamura S. 2009. Nuclear hormone receptor activity of polybrominated diphenyl ethers and their hydroxylated and methoxylated metabolites in transactivation assays using Chinese hamster ovary cells. Environ Health Perspect 117:1210–1218.

Lacorte S, Ikonomou MG. 2009. Occurrence and congener specific profiles of polybrominated diphenyl ethers and their hydroxylated and methoxylated derivatives in breast milk from Catalonia. Chemosphere 74:412–420.

Lagalante AF, Oswald TD, Calvosa FC. 2009. Polybrominated diphenyl ether (PBDE) levels in dust from previously owned automobiles at United States dealerships. Environ Int 35:539–544.

Li J, Ma M, Wang ZJ. 2008. A two-hybrid yeast assay to quantify the effects of xenobiotics on thyroid hormone-mediated gene expression. Environ Toxicol Chem 27:159–167.

Malmberg T, Athanasiadou M, Marsh G, Brandt I, Bergmant A. 2005. Identification of hydroxylated polybrominated diphenyl ether metabolites in blood plasma from polybrominated diphenyl ether exposed rats. Environ Sci Technol 39:5342–5348.

Malmvarn A, Marsh G, Kautsky L, Athanasiadou M, Bergman A, Asplund L. 2005. Hydroxylated and methoxylated brominated diphenyl ethers in the red algae *Ceramium tenuicorne* and blue mussels from the Baltic Sea. Environ Sci Technol 39:2990–2997.

Martinez L, Polikarpov I, Skaf MS. 2008. Only subtle protein conformational adaptations are required for ligand binding to thyroid hormone receptors: simulations using a novel multipoint steered molecular dynamics approach. J Phys Chem B 112:10741–10751.

Meerts IATM, van Zanden JJ, Luijks EAC, van Leeuwen-Bol I, Marsh G, Jakobsson E, et al. 2000. Potent competitive interactions of some brominated flame retardants and related compounds with human transthyretin in vitro. Toxicol Sci 56:95–104.

Mercado-Feliciano M, Bigsby RM. 2008. Hydroxylated metabolites of the polybrominated diphenyl ether mixture DE-71 are weak estrogen receptor-alpha ligands. Environ Health Perspect 116:1315–1321.

Nguyen TH, Goss K-U, Ball WP. 2005. Polyparameter linear free energy relationships for estimating the equilibrium partition of organic compounds between water and the natural organic matter in soils and sediments. Environ Sci Technol 39:913–924.

Qiu XH, Bigsby RM, Hites RA. 2009. Hydroxylated metabolites of polybrominated diphenyl ethers in human blood samples from the United States. Environ Health Perspect 117:93–98.

Qiu XH, Mercado-Feliciano M, Bigsby RM, Hites RA. 2007. Measurement of polybrominated diphenyl ethers and metabolites in mouse plasma after exposure to a commercial pentabromodiphenyl ether mixture. Environ Health Perspect 115:1052–1058.

Routti H, Letcher RJ, Chu SG, Van Bavel B, Gabrielsen GW. 2009. Polybrominated diphenyl ethers and their hydroxylated analogues in ringed seals (*Phoca hispida*) from Svalbard and the Baltic Sea. Environ Sci Technol 43:3494–3499.

Schüürmann G, Ebert RU, Chen JW, Wang B, Kuhne R. 2008. External validation and prediction employing the predictive squared correlation coefficient—test set activity mean vs training set activity mean. J Chem Inf Model 48:2140–2145.

Sippl W. 2002. Development of biologically active compounds by combining 3D QSAR and structure-based design methods. J Comput Aid Mol Des 16:825–830.

Soderholm AA, Lehtovuori PT, Nyronen TH. 2005. Three-dimensional structure-activity relationships of nonsteroidal ligands in complex with androgen receptor ligand-binding domain. J Med Chem 48:917–925.

Todeschini R, Consonni V. 2000. Handbook of Molecular Descriptors. Weinheim, Germany:Wiley-VCH.

U.S. Environmental Protection Agency. 2009. Download EPI SuiteTM v4.0. Available: http://www.epa.gov/oppt/exposure/pubs/episuitedl.htm [accessed 30 August 2009].

Valadares NF, Castilho MS, Polikarpov I, Garratt RC. 2007. 2D QSAR studies on thyroid hormone receptor ligands. Bioorgan Med Chem 15:4609–4617.

Wan Y, Wiseman S, Chang H, Zhang XW, Jones PD, Hecker M, et al. 2009. Origin of hydroxylated brominated diphenyl ethers: natural compounds or man-made flame retardants? Environ Sci Technol 43:7536–7542.

Wold S, Sjostrom M, Eriksson L. 2001. PLS-regression: a basic tool of chemometrics. Chemometr Intell Lab 58:109–130.

Wu GS, Robertson DH, Brooks CL, Vieth M. 2003. Detailed analysis of grid-based molecular docking: a case study of CDOCKER—a CHARMm-based MD docking algorithm. J Comput Chem 24:1549–1562.

Zhao YY, Tao FM, Zeng EY. 2008. Theoretical study on the chemical properties of polybrominated diphenyl ethers. Chemosphere 70:901–907.

Zhou T, Taylor MM, DeVito MJ, Crofton KA. 2002. Developmental exposure to brominated diphenyl ethers results in thyroid hormone disruption. Toxicol Sci 66:105–116.